# INFRARED HETERODYNE RADIOMETER FOR AIRBORNE ATMOSPHERIC TRANSMITTANCE MEASUREMENTS*

J. M. Wolczok, R. A. Lange, and A. J. DiNardo

Eaton Corporation, AIL Division, Melville, NY 11747

## SUMMARY

An infrared heterodyne radiometer (IHR) with an optical bandwidth of $10^{-3}$ $cm^{-1}$ was used to measure atmospheric transmittance at selected hydrogen fluoride (2.7 μm) and deuterium fluoride (3.8 μm) laser transitions. The IHR was installed aboard a KC-135 aircraft for an airborne atmospheric measurements program that used the sun as a backlighting source for the transmission measurements. The critical components are: a wideband indium antimonide (InSb) photomixer, a CW HF/DF laser LO, a radiometric processor, and a 1900K blackbody reference source. The measured heterodyne receiver sensitivity (NEP) is 1.3 x $10^{-19}$ W/Hz, which yields a calculated IHR temperature resolution accuracy of $\Delta T_S/T_S = 5 \times 10^{-3}$ for a source temperature of 1000K and a total transmittance of 0.5. Measured atmospheric transmittance at several wavelengths and aircraft altitudes from 9.14 km (30,000 ft) to 13.72 km (45,000 ft) were obtained during the measurements program and have been compared with values predicted by the AFGL Atmospheric Line Parameter Compilation.

## INTRODUCTION

One of the critical issues in the consideration of HF and DF laser transmission is the atmospheric molecular absorption. Although molecular absorption calculations have been carried out in the 2 to 5 μm region (ref. 1), limited ground-based field measurements (ref. 2) and no high altitude measurements have been previously reported.

---

*Program sponsored by Air Force Weapons Laboratory, Air Force Systems Command, Kirtland AFB, New Mexico under Contract F29601-76-C-0045.
Captain Terrence F. Deaton of the Air Force Weapons Laboratory was instrumental in assembling and conducting the entire flight measurements program.

A high altitude atmospheric measurements program was carried out by the Air Force Weapons Laboratory wherein the transmittance characteristics at the lasing transitions of hydrogen fluoride (HF) and deuterium fluoride (DF) lasers have been measured. In particular, measurements were carried out using a KC-135 aircraft platform at a variety of altitudes. Atmospheric transmittance along a path from a KC-135 aircraft platform to the sun was measured using the same technique previously employed to measure the high altitude transmission at $C^{12}O_2^{16}$ laser wavelengths (ref. 3). These measurements were carried out on the $P_2(7)$, $P_2(6)$, $P_2(5)$, $P_2(4)$, $P_2(3)$, and $P_1(4)$ transitions (2.8706 to 2.6401 μm) of the HF laser and the $P_3(9)$, $P_3(8)$, $P_3(7)$, $P_3(6)$, $P_2(9)$, $P_2(8)$, $P_2(7)$, $P_2(6)$, and $P_2(5)$ transitions (3.9654 to 3.698 μm) of the DF laser. The measurement results indicate a unity atmospheric transmittance on all of the DF laser transitions, and a generally lower transmittance than predicted for the HF laser transitions.

The IHR measured atmospheric transmittance within a spectral bandwidth of $10^{-3}$ $cm^{-1}$ about all of the HF and DF laser transitions. The measured receiver sensitivity (NEP) of the IHR is $1.3 \times 10^{-19}$ W/Hz, which yields a calculated IHR temperature resolution accuracy of $\Delta T_S/T_S = 5 \times 10^{-3}$ for source temperatures, $T_S$ = 1000K and transmittance $\alpha = 0.5$. Measurement accuracies near 0.5 percent have been calculated at HF and DF laser wavelengths.

## IHR OPTICAL TRAIN

The IHR optical train, shown in figure 1, consists of an objective lens that brings incident solar or calibration blackbody radiation to a focus, where it is Dicke switched (alternately referenced to an ambient temperature blackbody) by a motor-driven chopper wheel. The chopper wheel, which serves as the ambient blackbody, is coated with high-emissivity paint and held at a fixed reference temperature. The radiance passing through the chopper, and that emitted by the chopper blade, is collected and focused onto the PV:InSb photomixer by a relay lens. A plane-parallel beam from the local oscillator laser is directed onto the photomixer by a small injection mirror located directly behind the relay lens.

The optical Dicke switch is located at the focal point of the objective lens in order to provide square wave chopping of the sources, with a duty cycle of 50 percent. The position of the Dicke switch is electronically monitored by chopping an auxiliary light source to provide a synchronizing signal for the radiometric processor. This sync signal is sent to the electronics console, in the form of synchronizing pulses, so that detection can be synchronous with the Dicke switch position.

Provisions were made for temperature calibration of the IHR output with respect to a 300K and a 1900K blackbody calibration source. Since the unattenuated solar temperature is approximately 5750K (ref. 4), the use of a 1900K calibration blackbody (rather than 1300K) provided improved IHR measurement accuracy at temperatures greater than 1300K due to reduced extrapolation of the calibration signals. The IHR internal calibration sources can be inserted by using a flip mirror ahead of the objective lens.

The photomixer responds to the incident radiation energy at infrared frequencies above and below the local oscillator frequency and is band-limited by IF filters. This detected signal is amplified and processed (ref. 5). The frequency resolution is fixed at twice the IF bandwidth and, therefore, the IHR can provide an extremely high spectral resolving capability. Indeed, the present instrument has provision for a 50-MHz IF filter that yields an infrared spectral resolution of $3 \times 10^{-3}$ $cm^{-1}$ at $\lambda = 2.7$ μm. The necessity for such high spatial resolution is evident when one considers the extremely active and discrete line spectra of atmospheric species in the 2 to 5 μm region. For the intended measurement, the IHR instrument must have a spectral resolution that is comparable with the laser line resolution in order to measure a meaningful atmospheric transmittance.

The IHR optical system is shown in figure 2. The calibration insertion mirror can be seen adjacent to the objective lens. This mirror, together with the 300K calibration blackbody, can be positioned remotely from the electronics control console. The unit is RFI shielded, and all power leads enter the optical package via an RFI filter box. These precautions have been taken to ensure minimum interference from the aircraft environment and the HF (DF) laser LO, which is potentially a major source of RF interference.

Solar radiation is brought into the radiometer via an optical tracking system. The tracker is a video system with 30-cm (12-in.) diameter primary and secondary mirrors. The target acquisition is manual, and the control is then handed over to an on-board computer. Separate optical paths are used for: (1) the visible light to the video camera, and (2) the infrared radiation to the IHR. The "bicolor" window consists of a 15 cm (6 in.) x 25 cm (10 in.) quartz window for the visible radiation, and a 10 cm (4 in.) x 25 cm (10 in.) germanium window for the infrared radiation. The unobscured field of view of the tracker is approximately $\pm 6^{\circ}$ in azimuth and $0^{\circ}$ to $45^{\circ}$ in elevation.

## IHR ELECTRONICS

Since the IHR uses an ambient temperature reference (the Dicke switch chopper wheel), direct null-balanced radiometer operation is not possible when observing hot sources such as the sun. The method employed to deal with these hot sources is the utilization of gain modulation in the radiometer (ref. 5). The gain modulation circuitry alters the system gain during alternate phases of

the Dicke switch cycle, thereby adjusting that portion of the detected signal that represents the reference thermal energy. This enables null-balance operation of the IHR for source temperatures that are much larger than the reference temperature. Gain modulation is achieved by electronically switching a fixed attenuator into the null-balancing loop of the synchronous detector at the Dicke switch rate. The IHR temperature resolution with gain modulation is identical to that obtained when the IHR is null balanced by means of a reference temperature that is equal to the source temperature. Therefore, no degradation in IHR performance is experienced due to any variations in laser LO power or IHR gain which occur slowly compared to the Dicke switch rate.

The IF output from the InSb photomixer is amplified and processed in an AIL 777 Radiometer Processor. The processor provides synchronous detection that employs the self-balancing gain modulation technique (ref. 3). A simplified block diagram of the processor is shown in figure 3. The output of the InSb photomixer is IF amplified, detected, and decommutated. The output level obtained while viewing the chopper wheel reference temperature is used to maintain a fixed system gain by means of feedback to the AGC amplifier located ahead of the square-law detector. The decommutated output is used to provide separate control of the processor gains, when viewing either the reference chopper wheel or the external source/calibration blackbody. The output of the synchronous detector is driven to a null balance by means of a variable digital attenuator which controls the video gain in the processor when viewing the reference source.

Temperature range and resolution control of the processor output are available to maximize the resolution of the digital output for any range of expected source temperatures. The digital attenuator output, which is directly proportional to input source radiance, has 1024 discrete steps.

## IHR PHOTOMIXER AND LASER LO

A photovoltaic InSb detector with an active area of $1.5 \times 10^{-4}$ $cm^2$ is used as the IHR photomixer. The reverse shunt resistance of the InSb detector is of the order of 3 megohms, resulting in low values of photomixer dark current ($I_D$), and the requirement for an IF preamplifier that operates from a relatively high source impedance. Frequency response measurements were carried out with the InSb photomixer at 77K in the IHR configuration. The measured 3-dB cutoff frequency was $f_c$ = 50 MHz for a reverse bias voltage of $V_B$ = -600 mV, and increased to $f_c$ = 60 MHz for $V_B$ = -800 mV. The laser LO induced photocurrent was about 0.15 mA compared to a dark current of approximately 0.02 mA.

The CW HF (DF) laser is of the basic design which was initially reported by Hinchen (ref. 6), with appropriate modifications for airborne use. The

grating-tunable, flowing-gas, water-cooled laser has an optical cavity which is 30 cm long and provides a $TEM_{00}$ transverse mode. A stabilization loop is employed to continuously adjust the cavity length and maintain the laser tuned on the center of the selected transition.

## IHR TEMPERATURE RESOLUTION ACCURACY

The IHR temperature resolution, $T_s$, is defined as the maximum change in source temperature for which no change in output signal-to-noise ratio is observable. The IHR temperature resolution is given (ref. 4) by

$$\Delta T_s = \frac{k^2 I_s^2}{h^2 \nu^2} \cdot \frac{[\exp(h\nu/kT_s)-1]^2}{\alpha \exp(h\nu/kT_s)} \cdot \sqrt{\frac{K}{B\tau}} \left[ \frac{2h\nu\alpha}{k[\exp(h\nu/kT_s)-1]} + \int_{f_1}^{f_2} \frac{NEP(f)\,df}{kB} \right] \tag{1}$$

where $\alpha$ is the transmittance of the media and optics between thermal source and infrared photomixer, K is the sensitivity constant which is 2 for a Dicke-type receiver, $T_s$ is the source temperature, B is the predetection (IF) bandwidth, $\tau$ is the postdetection integration time for a pure integration, $\nu$ is the infrared frequency, k is Boltzmann's constant, h is Planck's constant, and f is the IF frequency.

The receiver sensitivity (NEP) for a heterodyne receiver with a photovoltaic photomixer is given (ref. 7) by

$$\left.\begin{aligned} NEP &= \int_{f_1}^{f_2} NEP(f)\,df \\ NEP(f) &= \frac{h\nu}{\eta}\left\{1 + 2K\frac{(T_m + T'_{IF})}{q I_o} G_D [1 + (f/f_c)^2]\right\} = \frac{h\nu}{\eta'} \end{aligned}\right\} \tag{2}$$

where $\eta$ is the photomixer quantum efficiency, $T_m$ is the photomixer temperature, $T'_{IF}$ is the effective input noise temperature of the IF amplifier, $G_D$ is the reverse shunt conductance of the photomixer, $I_o$ is the LO induced photocurrent, $f_c$ is the 3-dB cutoff frequency of the photomixer, and $\eta'$ is the effective receiver quantum efficiency.

The temperature resolution of the IHR is affected by optic losses, spherical aberration, coma, astigmatism, lens emissivity, lens temperature, amplitude fluctuations that occur faster than the Dicke switch rate, and the obscuration due to the LO injection mirror. The calculated resolution accuracy, $\Delta T_s/T_s$, of a gained-modulated Dicke-switched IHR is given in figure 4 for $\lambda = 3$ μm, $\beta\tau = 5 \times 10^9$, and a heterodyne receiver NEP of $1.3 \times 10^{-19}$ W/Hz with the transmittance $\alpha$ as a parameter. For a source temperature of 1000°C and $\alpha = 10$ percent, the calculated temperature resolution accuracy is $\Delta T_s/T_s \simeq 1.6 \times 10^{-2}$, while for $\alpha = 100$ percent, the resolution accuracy improves to $\Delta T_s/T_s \simeq 1.6 \times 10^{-3}$. For the solar viewing case ($T_s \simeq 5750$K for 100 percent atmospheric transmittance), the calculated temperature resolution accuracy is $\Delta T_s/T_s = 9 \times 10^{-5}$ for a transmittance of $\alpha = 0.25$.

## IHR TEMPERATURE RESOLUTION

The solar radiation, $P(\nu)$, collected at the IHR is the product of the incident unattenuated solar radiation, $P_o$, and an exponential attenuation term due to the intervening atmospheric losses. Therefore

$$P(\nu) = P_o \exp\left[-k_\alpha(\nu)\, n\sec\theta\right] \tag{3}$$

where $k_\alpha(\nu)$ is the atmospheric attenuation coefficient at selected laser LO frequency, h is the height of atmosphere, $\theta$ is the zenith angle of the sun, and nsec $\theta$ is the path length of sunlight through the atmosphere.

The IHR output voltage is proportional to the collected source energy. The slope of the logarithm of $P(\nu)$ plotted against sec $\theta$ is $-k_\alpha(\nu)\, h$, and $\exp\left[-k_\alpha(\nu)h\right]$ is the total vertical path transmittance $\alpha$ (ref. 2, 4, 8, and 9). The vertical path atmospheric transmittance can therefore be experimentally determined by measuring the solar radiance while tracking the sun as the earth

turns. The measurements can be carried out at different laser local oscillator frequencies, solar angles, and altitudes.

When observing a thermal source that fills the IHR field of view, the postdetection signal-to-noise ratio is given (ref. 4) by

$$SNR = \frac{\eta' \nu (B\tau)^{1/2}}{e^{h\nu/kT_s} - 1} \tag{4}$$

Equation (4) can be rewritten as

$$\alpha = \gamma \frac{S}{N} \tag{5}$$

where $\gamma$ is a constant for a fixed set of measurement parameters. Differentiating $\alpha$ with respect to S yields

$$d\alpha = \frac{\gamma}{N} ds \tag{6}$$

The minimum detectable signal change occurs when ds = N. Therefore, the accuracy of the measurement of atmospheric transmittance is given by

$$\frac{d\alpha}{\alpha} = \frac{1}{SNR} \tag{7}$$

For a typical solar observation, where $T_s$ = 5000K, B = 50 MHz, $\tau$ = 10 s, B = 5 x $10^9$, $\eta'$ = 0.2, and a total atmospheric transmittance of $\alpha$ = 0.5 from sea level to 30 km during midlatitude summer at $\lambda$ = 3 μm, the SNR of an IHR observing the solar disc at zenith is calculated to be SNR = 2000, and the expected accuracy of the measurement is $d\alpha/\alpha$ = 0.05 percent.

Calculations have also been carried out to determine the obtainable IHR power resolution. The resolution is a function of the effective system quantum efficiency, the calibration blackbody temperature, and the $B\tau$ product of the IHR. The smallest calculated change in irradiance that can be measured for a given input radiance is given in figure 5. It should be noted that the overall system quantum efficiency, $\eta'$, depends on both the quantum efficiency of the infrared photomixer and the heterodyne mixing efficiency which is determined by the IHR optical configuration and the photomixer size.

The PV:InSb photomixer used in the IHR has a quantum efficiency of approximately 75 percent. The IHR system loss factor is approximately 3 dB due

to both optics losses and mixing inefficiency. This results in an overall IHR system quantum efficiency of $\eta' = 37$ percent. As seen from figure 5, a 1900K blackbody source will yield a resolution of about 3 parts per 1000 as compared with a resolution of about 10 parts per 1000 for a 1300K source temperature for $\lambda = 2.9$ μm and $B\tau = 10^9$.

## CALCULATED AND MEASURED ATMOSPHERIC TRANSMITTANCE DATA

Calculations and measurements have been carried out to determine the expected atmospheric transmittance at various altitudes for a number of selected HF and DF laser transitions. As an example, the calculated transmittance for a midlatitude winter model (with no aerosols present) is given in table I for the $P_2(7)$ transition ($\lambda = 2.8706$ μm) of the HF laser (ref. 1). The transmittance values have been calculated for the optical path between the edge of the atmosphere and the selected aircraft altitude, with the solar viewing angle as a variable parameter. As can be seen in table I, the calculated transmittance for the $P_2(7)$ transition of HF increases with increasing aircraft altitude.

The IHR flight measurements program occurred between July, 1977 and January, 1978. During the flight tests, atmospheric pressure, temperature, and humidity data were obtained from point analyses supplied by the USAF Environmental Technical Applications Center (ETAC). ETAC has developed a linear regression model (ref. 10) which estimates water vapor levels above the $-40^{\circ}$ level, at which standard operational rawinsondes fail. The ETAC model is based on a series of actual soundings by the Naval Research Laboratory. Each point analysis is based on the data from a particular rawinsonde launch. For early morning flights over New Mexico, the 1200Z (5 A.M. MST) Albuquerque rawinsonde data and corresponding point analysis data were used to compute the transmittance. In a few instances, soundings from El Paso and Midland, Texas, and Grand Junction, Colorado were also used. A sample profile showing the comparison between the point analysis and the rawinsonde data of the water vapor profile is shown in figure 6. As can be seen, the agreement is excellent and the water vapor pressure at 30,000 feet is about two orders of magnitude lower than the water vapor pressure between ground level and 1.83 km (6,000 ft).

The calculated transmittance values do not account for aerosol scattering or absorption, which might have a small effect on the transmittance at the altitudes of interest. The calculated water vapor absorption, even for relatively high humidity conditions, is almost negligible for altitudes above 12.19 km (40,000 ft) for all the laser transitions which were measured. The molecular absorption is due chiefly to $CO_2$, with significant $N_2O$ absorption only on the $P_2(7)$ transition of the HF laser. The agreement of the measurements with the calculated transmittance values is generally good. Because of noise problems, due to poor HF laser stability, the IHR signal-to-noise ratio

for unattenuated solar radiation was about 30:1 and, therefore, it was difficult to measure transmission of less than $\alpha = 0.10$.

Measured atmospheric transmittance data for several selected HF laser transitions are given in figures 7 and 8. Tables II, III and IV summarize some of the measured atmospheric transmittance data for the $P_2(6)$, $P_2(7)$, and $P_1(4)$ transitions of the HF laser.

## CONCLUSION

An infrared heterodyne radiometer has been designed, developed, and fabricated for use on a KC-135 aircraft. The extremely narrow bandwidth ($10^{-3}$ $cm^{-1}$) IHR has been designed to operate at the HF/DF laser transitions and exhibits the following characteristics:

| | |
|---|---|
| Wavelength | 2.7 to 3.8 μm |
| Receiver type | Gain modulated, Dicke-switched, heterodyne |
| Receiver field of view | ≈ 2 mrad |
| Receiver sensitivity (NEP) | $1.3 \times 10^{-19}$ W/Hz |
| Dicke switch rate | 500 to 2000 Hz, selectable |
| IF bandwidth | 50 or 100 MHz, selectable |
| Integration time | 0.1, 0.5, 1.3, or 10 s selectable |
| Reference temperature | Ambient |
| Calibration temperature | 1000 to 1900K, ambient |
| Blackbody calibration accuracy | ≈ 1 percent |
| Blackbody calibration | ≈ 0.25 percent, long term<br>≈ 0.05 percent, short term |
| Overall measurement accuracy | 0.5 to 0.1 percent |

During the design and development of the IHR, consideration was also given to operation at other infrared wavelengths. Although the IHR is presently being used for solar and atmospheric transmittance measurements, there are a number of other potential applications for this unique instrument. The

infrared spectrum is rich in absorption (emission) phenomena in the 2 to 12 μm spectral region. The narrow bandwidth IHR offers the potential of spectral overlap with selected signature lines to permit the remote detection and monitoring of various atmospheric constituents. Previous atmospheric measurements near $\lambda = 10$ μm (ref. 8) have resulted in the remote determination of the concentration profile of atmospheric ammonia and ozone.

TABLE I. CALCULATED ATMOSPHERIC TRANSMITTANCE FOR $P_2(7)$ TRANSITION OF HF LASER FOR MIDLATITUDE WINTER (NO AEROSOL) AND $\theta$ = SUN'S ANGLE FROM ZENITH

| Altitude (km) | Transmittance $\theta = 80^o$ | $\theta = 70^o$ | $\theta = 60^o$ | $\theta = 50^o$ |
|---|---|---|---|---|
| 10 | 0.9552 | 0.9770 | 0.9842 | 0.9877 |
| 9 | 0.9348 | 0.9664 | 0.9769 | 0.9820 |
| 8 | 0.8984 | 0.9471 | 0.9635 | 0.9715 |
| 7 | 0.8241 | 0.9064 | 0.9350 | 0.9491 |
| 6 | 0.6791 | 0.8216 | 0.8742 | 0.9007 |

TABLE II. ZENITH TRANSMITTANCE FOR $P_2(6)$ TRANSITION OF HF LASER ($\lambda$ = 2.8318 μm)

| Altitude | Measured transmittance | Calculated transmittance |
|---|---|---|
| 9.45 km (31,000 ft) | 0.924 | 0.918 |
| 10.67 km (35,000 ft) | 0.954 | 0.939 |
| 11.28 km (37,000 ft) | 0.987 | 0.968 |
| 11.89 km (39,000 ft) | 0.970 | 0.954 |
| 12.50 km (41,000 ft) | 0.982 | 0.964 |
| 13.72 km (45,000 ft) | 1.00 | 0.974 |

TABLE III. ZENITH TRANSMITTANCE FOR $P_2(7)$ TRANSITION OF HF LASER ($\lambda$ = 2.8706 μm)

| Altitude | Measured transmittance | Calculated transmittance |
|---|---|---|
| 10.67 km (35,000 ft) | 0.993 | 0.995 |
| 11.28 km (37,000 ft) | 1.0 | 0.993 |
| 11.89 km (39,000 ft) | 1.0 | 0.996 |
| 12.50 km (41,000 ft) | 1.0 | 0.998 |
| 13.72 km (45,000 ft) | 1.0 | 0.998 |

TABLE IV. ZENITH TRANSMITTANCE FOR $P_1(4)$ TRANSITION OF HF LASER ($\lambda$ = 2.6401 μm)

| Altitude | Measured transmittance | Calculated transmittance |
|---|---|---|
| 10.97 km (36,000 ft) | 0.55 | 0.975 |
| 12.50 km (41,000 ft) | 0.74 | 0.99 |
| 13.72 km (45,000 ft) | 0.85 | 0.995 |

## REFERENCES


1. McClatchey, R. A.; and Selby, J. E.: Atmospheric Attenuation of HF and DF Laser Radiation. Air Force Cambridge Research Lab., Report No. AFCRL-72-0312, May 1972.

2. Snemabukuro, F. I. et al: Atmospheric Transmission Measurements at HF and DF Laser Wavelengths. Appl. Opt. vol. 15, no. 5, May 1976, pp. 1115-1117.

3. Peyton, B. J.; Hoell, J. M.; Lange, R. A.; Savage, M. G.; and Allario, F.: Remote Airborne Measurements of Stratospheric Ozone. Proc. of Laser '79 Conference, Orlando, Fla. 1979.

4. Murcray, F. R.; Murcray, D. G.; and Williams, W. J.: The Spectral Radiance of the Sun from 4 μm to 5 μm. Appl. Optics, vol. 3, no. 12, Dec. 1964, pp. 1373-1377.

5. Peyton, B. J. et al: An Infrared Heterodyne Radiometer for High-Resolution Measurements of Solar Radiation and Atmospheric Transmission. IEEE J. Quant. Elec., QE-11, Aug. 1975.

6. Hinchen, J. J.: Operation of a Small Single-Mode Stable CW Hydrogen Fluoride Laser, J. App. Phys., no. 45, 1974, p. 1818.

7. Peyton, B. J. et al: High Sensitivity Receiver for Infrared Laser Communication. IEEE J. Quant. Electr., QE-8, Feb. 1972, pp. 252-263.

8. Peyton, B. J. et al: Infrared Heterodyne Spectrometer Measurements of the Vertical Profile of Tropospheric Ammonia and Ozone. AIAA Conference, Los Angeles, Ca., Jan. 1977.

9. King, S. R.; Hodges, D. T.; Hartwick, T. S.; and Baker, D. H.: High Resolution Atmospheric-Transmission Measurements Using a Laser Heterodyne Radiometer, Appl. Opt., vol. 112, June 1973, p. 1106.

0. Mendenhall, L. D.; Stanton, T. E.; and Henderson, H. W.: A Model for Describing the Atmospheric Water Vapor Profile above the -40°C Temperature Level. USAF Environmental Technical Applications Center Report 7584, Aug. 20, 1975.

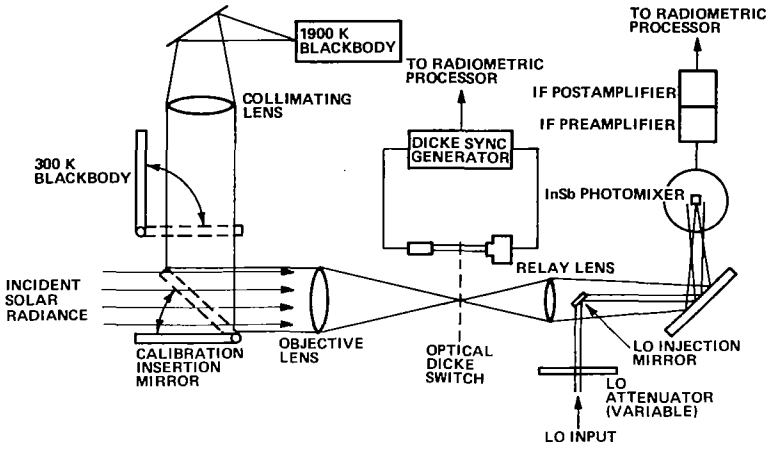


Figure 1.- Diagram of IHR optical train.

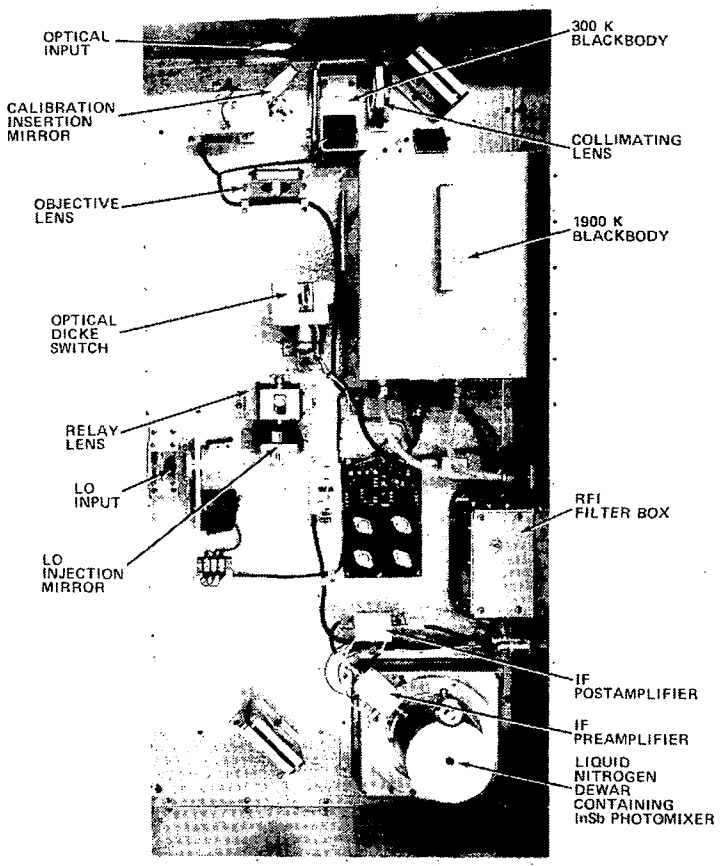


Figure 2.- Top view of IHR optical system.

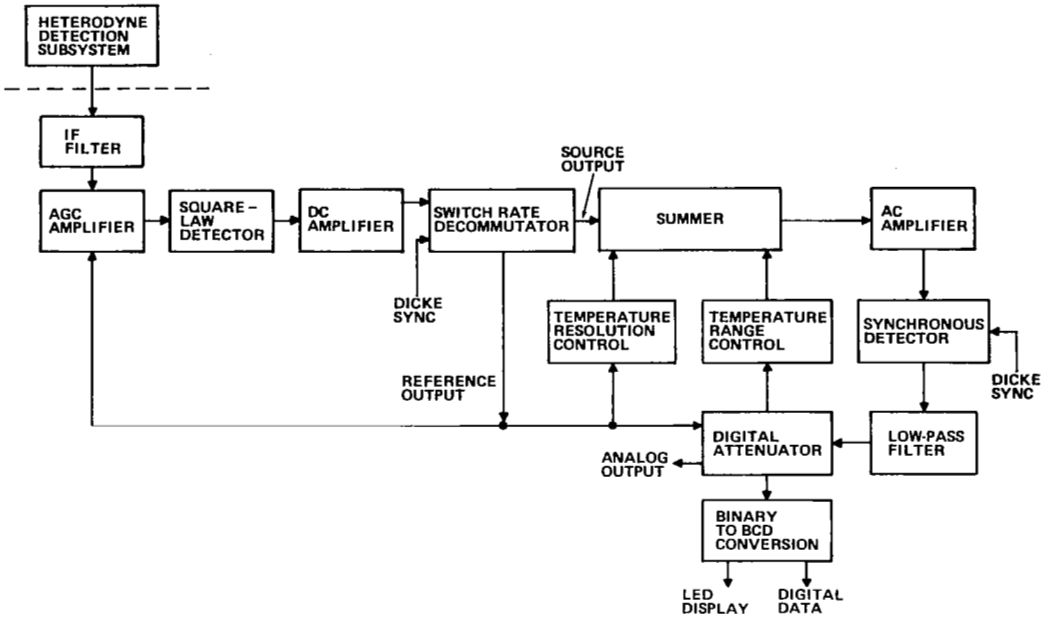


Figure 3.- Block diagram of IHR processor with self balancing gain modulation.

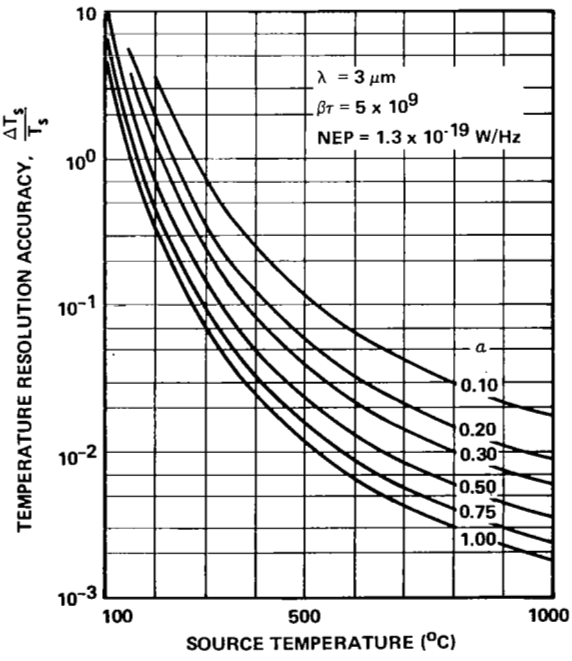


Figure 4.- Calculated IHR temperature resolution.

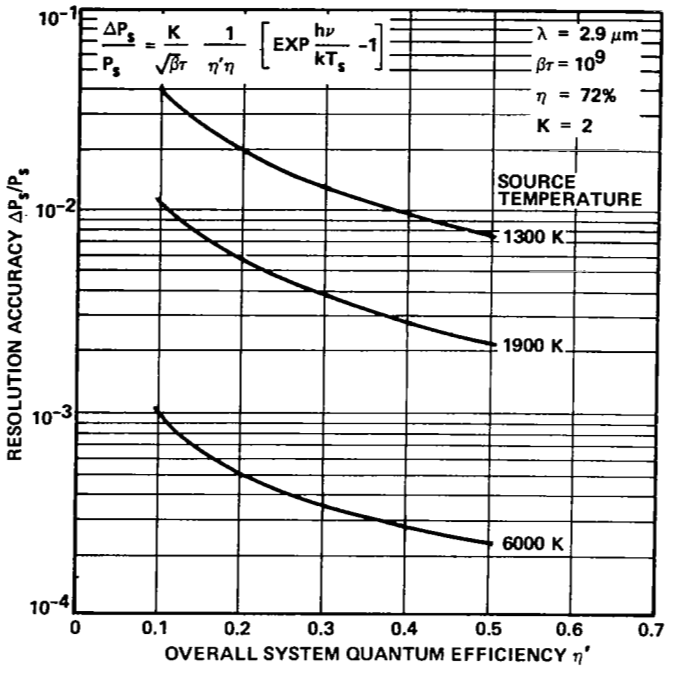


Figure 5.- Calculated IHR resolution accuracy.

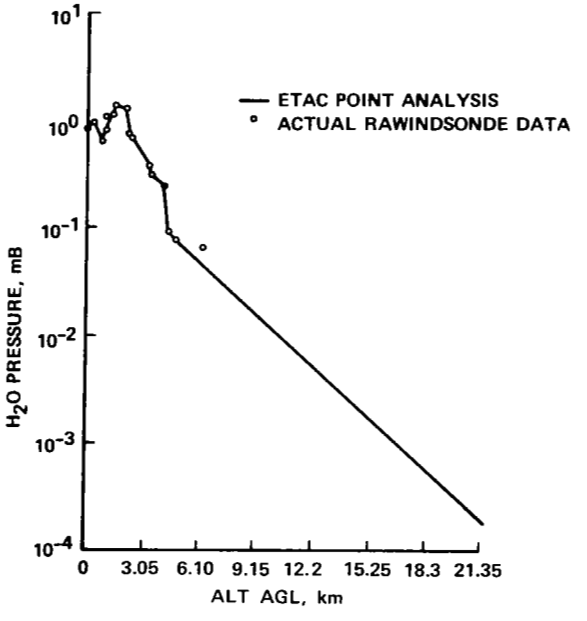


Figure 6.- ETAC point analysis water vapor profile compared to actual rawinsonde data for sounding of Bismarck, ND 1700 MST, 7 Jan. 1978.

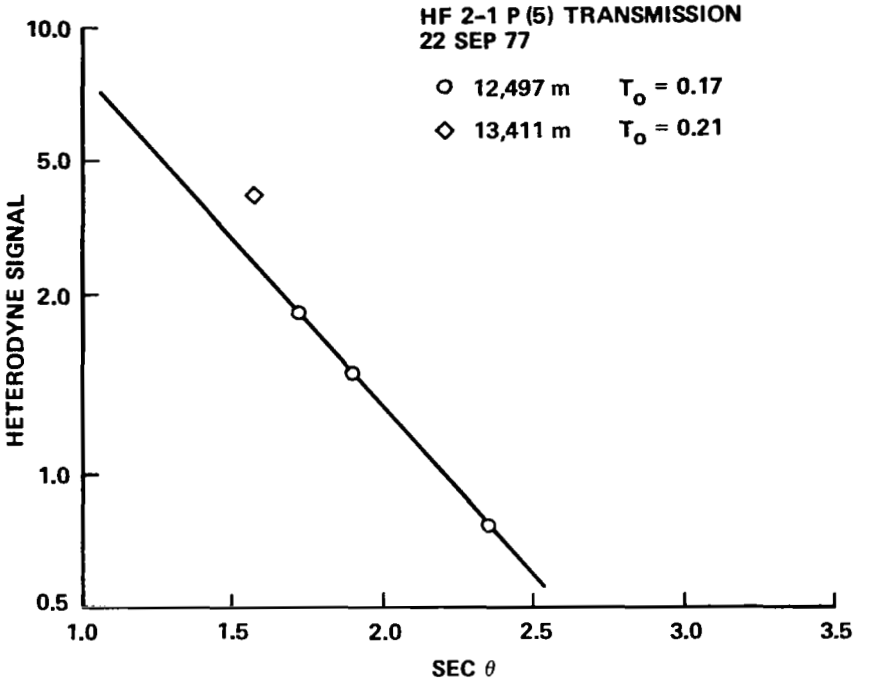


Figure 7.- HF $P_2(5)$ transmission plot for altitudes shown over Rapid City, SD, 22 Sept. 1977.

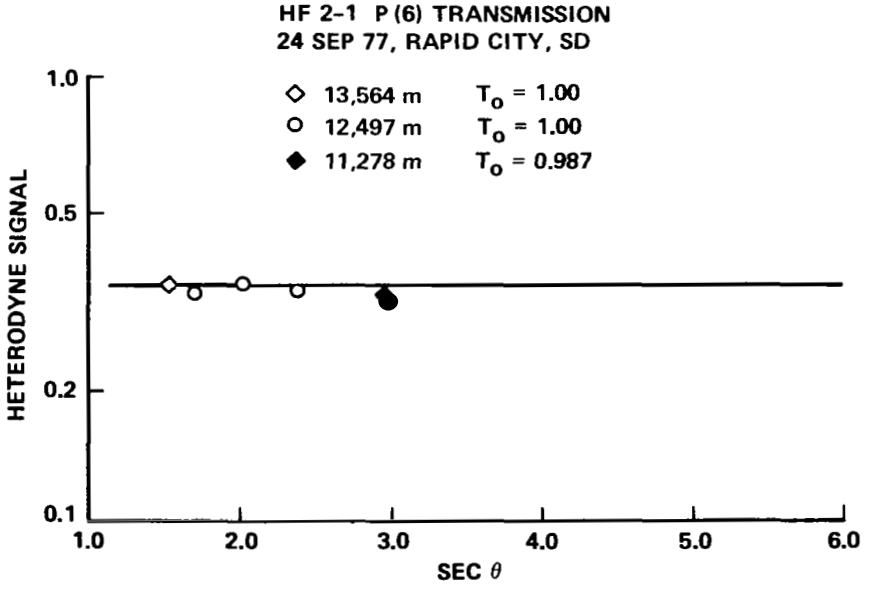


Figure 8.- HF $P_2(6)$ transmission plot for altitudes shown over Rapid City, SD, 24 Sept. 1977.